(6) W. J. Hehre, W. A. Lathan, R. Ditchfield, M. D. Newton, and J. A. Pople, Quantum Chemistry Program Exchange, Indiana University, Bloomington, Indiana.
(7) The MWH calculations were performed using Clementi ζ's for the orbital exponent: E. Clementi, *IBM J. Res. Dev.*, **9**, 2 (1965).
(8) The ionization potentials were calculated for the isolated radicals by the MWH method.
(9) In our original paper the term CI referred to mixing of a ground state and a diexcited configuration and, on the basis of this definition, CI was stated to be unimportant in nonpolar and important in polar 1,3 shifts. In terms of the more general definition of CI, e.g., a total wave function written as a linear combination of more than one Slater determinant, it can be said that CI is important in both nonpolar and polar 1,3 shifts. For this clarification see footnote 6 in ref 2c.
(10) For example, see Figure 2a in ref 2c.
(11) D. W. Turner, *Adv. Phys. Org. Chem.*, **4**, 31 (1966).

Localized Molecular Orbitals for Polyatomic Molecules. II. Structural Relationships and Charge Distributions for Open Boron Hydrides and Ions

J. H. Hall, Jr., D. A. Dixon, D. A. Kleier, T. A. Halgren, L. D. Brown, and W. N. Lipscomb*

Contribution from the Department of Chemistry, Harvard University, Cambridge, Massachusetts 02138. *Received December 12, 1974*

Abstract: Wave functions calculated in the partial retention of diatomic differential overlap (PRDDO) approximation are presented for B_8H_{12}, B_8H_{14}, $B_8H_{13}^-$, B_9H_{15}, $B_9H_{14}^-$, $B_{10}H_{14}$, $B_{10}H_{14}^{2-}$, $B_{10}H_{13}^-$, $B_{11}H_{13}^{2-}$, $C_2B_7H_{13}$, $C_2B_9H_{12}^-$, and $C_2B_{10}H_{13}^-$. The wave functions are analyzed in terms of the ground state charge distribution. Mulliken overlap populations, atomic and group charges, dipole moments, and ionization potentials are presented for these molecules. We compare reactivity predictions for electrophilic and nucleophilic attack at boron based on three different criteria: inner shell eigenvalues, group charges, and population sums over the highest occupied molecular orbitals. Localized molecular orbitals (LMO's) obtained using the Boys criterion are reported. The molecules are grouped into three families based on common structural features with B_8H_{12}, $B_{10}H_{14}$, and $B_{11}H_{13}^{2-}$ serving as parent molecules. Within each family, differences in LMO structure are correlated with differences in the geometrical structure and charge distribution.

We compared, in paper I,[1] the Edmiston-Ruedenberg (ER)[2] and Boys[3] localization criteria for a group of boranes and carboranes which ranged from B_2H_6 to 2,4-$C_2B_5H_7$ in size.[4] The two methods yielded identical localized bond models in nearly all cases, even though computationally the Boys procedure was found to be approximately 100 times faster for these molecules. The single difference occurred in 1,2-$C_2B_4H_6$, for which the ER criterion yielded a pair of open[5] three-center B-C-B bonds while the Boys structure displayed only central three-center bonds.[1]

We here apply the computationally efficient Boys method to a series of structurally related nido boranes and carboranes which contain from 8 to 12 boron and carbon atoms. The molecules and ions considered here fall into three main families for which B_8H_{12}, $B_{10}H_{14}$, and $B_{11}H_{13}^{2-}$ can serve as parent structures (Figure 1). With the aid of the localized orbitals, we examine the relationship of bonding patterns within the families. In addition, since the chemical behavior of these systems toward electrophiles and nucleophiles has not yet been extensively explored experimentally, we offer predictions, based on the ground state charge distributions, for relative reactivity in electrophilic and nucleophilic processes. The principal indicators employed for this purpose are Mulliken atomic[6] and group charges (see below) and inner-shell eigenvalues.[7] The self-consistent-field calculations upon which these predictions are based are minimum-basis-set Slater orbital calculations carried out in the recently introduced approximation of partial retention of diatomic differential overlap (PRDDO).[8]

Molecular Geometries. The geometries of B_8H_{12}, $B_8H_{13}^-$, B_9H_{15}, $B_9H_{14}^-$, $B_{10}H_{14}^{2-}$, $B_{10}H_{13}^-$, $B_{11}H_{13}^{2-}$, $C_2B_7H_{13}$, $C_2B_9H_{12}^-$, and $C_2B_{10}H_{13}^-$ were taken from, or extrapolated from, X-ray crystal structures,[9-18] and the geometry of $B_{10}H_{14}$ was taken from the neutron diffraction study.[19] Each set of crystallographic coordinates was idealized to the presumed molecular symmetry, and appropriate B-H_t distances (1.19 Å) were imposed to correct the systematic X-ray shortenings.[20] However, the facial proton in $C_2B_9H_{12}^-$ was left at its crystal structure B-H_t distance of 1.33 Å. Since the structure of B_8H_{14} is uncertain the geometries employed for B_8H_{14} are hypothetical and utilize B-H-B and B-B distances from B_8H_{12} and $B_8H_{13}^-$ (see below) together with B-H_t distances of 1.19 Å. The numbering schemes used throughout this paper are given in Figures 3-16. For clarity, one terminal hydrogen is omitted from each heavy atom. In order to compare more easily molecules within each family (Figure 1), each molecule has been numbered in accordance with the parent molecule for that family (thus, except for the parent molecules we have used a nonstandard numbering).[21]

SCF Calculations. As details of the PRDDO method are described elsewhere,[8] we give here only a brief account. The PRDDO method uses a Slater basis set and explicitly treats all electrons. No experimental parameters are employed, but certain contributions to the two-electron matrix are parameterized to reproduce ab initio matrix elements for a variety of small molecules.[8] Thus, PRDDO is a *nonempirical* molecular orbital method. For molecules of the size considered here, computing times are roughly 100 times smaller than those for the reference ab initio SCF calculations. Extensive comparisons[8c,22] of PRDDO results with those given by other methods have established that PRDDO is greatly superior to CNDO and INDO[23] and is comparable to STO-3G[24] in reproducing energy differences, charge distributions, dipole moments, and eigenvalues from reference ab initio minimum Slater basis set calculations. For this study, exponents for boron and attached hydrogens have been taken from optimized values for B_2H_6[25a] while exponents

Table I. Energy Analysis[a]

	B_8H_{12}	B_8H_{14}	$B_8H_{13}^-$	B_9H_{15}	$B_{10}H_{14}$	$B_{10}H_{13}^-$	$B_9H_{14}^-$	$B_{10}H_{14}^{2-}$	$B_{11}H_{13}^{2-}$	$C_2B_7H_{13}$	$C_2B_9H_{12}^-$	$C_3B_{10}H_{13}$
Nuclear repulsion energy	283.783	300.239	285.592	357.539	414.502	407.902	356.598	410.386	470.406	377.933	496.678	559.384
Kinetic energy	204.135	205.187	205.096	230.395	254.699	255.477	230.997	265.022	280.596	255.878	496.678	559.384
Nuclear attraction energy	−1036.022	−1070.679	−1052.276	−1243.006	−1412.80	−1412.293	−1253.358	−1431.954	−1609.651	−1344.974	−1709.764	−1893.682
Electron repulsion energy	343.890	359.923	356.773	424.510	488.816	494.639	435.740	510.809	579.782	455.328	602.887	673.991
Total energy	−204.214	−205.331	−204.815	−230.562	−254.797	−254.275	−230.022	−254.736	−278.867	−255.836		
Virial ratio ($-E/T$)	1.0004	1.0007	0.9986	1.0007	1.0004	0.9953	0.9958	0.9950	0.9938	0.9998	0.9979	0.9995
Highest occupied[b] MO eigenvalue	−0.365	−0.408	−0.111	−0.376	−0.416	−0.169	−0.162	0.063	0.057	−0.374	−0.164	−0.206
Lowest unoccupied MO eigenvalue	0.080	0.101	0.278	0.084		0.265	0.271	0.546	0.589	0.123	0.413	0.256

[a] All energies in atomic units (au). [b] For negative values, the absolute value corresponds to the ionization potential.

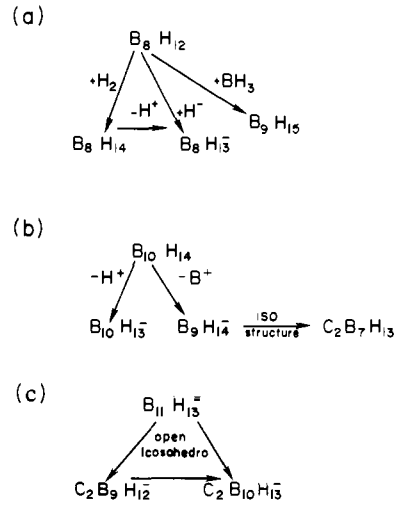

Figure 1. Schematic diagram showing structural relationships between members of the nido boranes and carboranes: (a) relationships of B_8H_{12}-like molecules; (b) relationships of $B_{10}H_{14}$-like molecules, $B_9H_{14}^-$ and $C_2B_7H_{13}$ are isostructural and isoelectronic; (c) $B_{11}H_{13}^{2-}$, $C_2B_9H_{12}^-$, and $C_2B_{10}H_{13}^-$ are icosahedra missing an apex.

for carbon and related hydrogens are based on optimized results for C_2H_6.[25b]

Tables I–III present the energy analysis for the systems not reported previously[22] and list Mulliken charges,[6] inner-shell eigenvalues for the first-row atoms, and dipole moments. Overlap populations[6] for the boron hydrides are given in Table IV except for B_8H_{12}, B_9H_{15}, $B_{10}H_{14}$, and $B_{10}H_{14}^{2-}$, for which values are reported elsewhere.[22,26]

Reactivity and Charge Distributions. Static reactivity indices have been quite successful in predicting the relative orders of nucleophilic and of electrophilic substitution in boron hydrides and carboranes.[26] Applicability of these indices necessarily requires that steric effects are minimal and that the relative rates are governed by formation of a transition state which is influenced principally by the initial ground state charge distribution. Previous comparisons for boranes and carboranes have shown that the PRDDO method yields charge distributions which agree very closely with those given by the reference SCF calculations.[22] The reactivity predictions presented here are based upon the relative values of inner-shell eigenvalues and of Mulliken atomic and group charges (Table II). Thus, boron atoms associated with the least negative inner-shell eigenvalues should be embedded in the largest concentrations of electronic charge[7] and hence are predicted to be most susceptible to electrophilic substitution. Although not always explicitly stated in the comparisons which follow, nucleophilic substitution is then expected to occur in the reverse order. A population analysis provides an alternative, and apparently more direct, means of assessing the distribution of electronic charge. However, Mulliken atomic charges incorporate a somewhat artificial partitioning of atomic overlap charge distributions and hence are of uncertain utility.[6] We calculate group charges for the first-row atoms by adding the charges of the terminal hydrogens and one-half the charge of attached bridge hydrogens to the atomic charge; thus, the group charges sum to the total electronic charge. The use of the group charges is expected to decrease the ambiguity resulting from the arbitrary division of overlap charge between atoms because there is less ultimate division of charge.

In order to test the presumed correlation between inner shell eigenvalues, ϵ_i, and the Mulliken atomic and group charges, q_i, linear least-squares fits were performed for the

Table II. PRDDO–SCF Inner Shell Eigenvalues, Atomic Charges, and Group Charges

Molecule	Atom	Eigenvalue[a]	Atomic charge[b]	Group charge[b]
B_8H_{12}	B_2	−7.567	−0.04	−0.09
	B_3	−7.595	0.00	−0.04
	B_1	−7.598	0.03	−0.02
	B_4	−7.610	0.08	0.01
	B_7	−7.655	0.08	0.08
B_8H_{14}	B_4	−7.572	−0.09	−0.14
	B_2	−7.565	−0.05	−0.11
	B_1	−7.586	−0.04	−0.07
	B_7	−7.663	0.08	0.06
	B_3	−7.668	0.18	0.17
$B_8H_{13}^-$	B_4	−7.316	0.02	−0.30
	B_2	−7.362	−0.06	−0.17
	B_1	−7.370	−0.02	−0.11
	B_3	−7.399	0.01	−0.09
	B_7	−7.500	0.13	0.03
B_9H_{15}	B_2	−7.568	−0.05	−0.11
	B_4	−7.595	0.00	−0.03
	B_1	−7.608	0.03	0.00
	B_3	−7.620	0.06	0.02
	B_9	−7.631	0.03	−0.06
	B_7	−7.684	0.11	0.09
$B_{10}H_{14}$	B_2	−7.576	−0.03	−0.08
	B_1	−7.592	0.02	−0.03
	B_5	−7.634	0.05	0.01
	B_6	−7.678	0.10	0.09
$B_{10}H_{13}^-$	B_5	−7.360	−0.04	−0.15
	B_2	−7.360	−0.04	−0.15
	B_4	−7.380	−0.06	−0.16
	B_1	−7.383	0.01	−0.09
	B_6	−7.385	0.04	−0.10
	B_3	−7.391	−0.02	−0.11
	B_7	−7.425	0.02	−0.10
	B_9	−7.428	0.06	−0.06
	B_8	−7.454	0.05	−0.04
	B_{10}	−7.485	0.03	0.01
$B_9H_{14}^-$	B_4	−7.349	−0.14	−0.24
	B_2	−7.367	−0.03	−0.14
	B_8	−7.384	0.11	−0.18
	B_1	−7.387	−0.01	−0.08
	B_5	−7.432	0.09	−0.01
	B_6	−7.473	0.04	−0.06
$B_{10}H_{14}^{2-}$	B_6	−7.156	−0.02	−0.34
	B_1	−7.185	−0.03	−0.19
	B_5	−7.208	0.00	−0.15
	B_2	−7.220	0.01	−0.13
$B_{11}H_{13}^{2-}$	B_2	−7.121	−0.07	−0.26
	B_7	−7.185	−0.04	−0.20
	B_{12}	−7.187	0.00	−0.16
	B_{10}	−7.189	0.03	−0.15
	B_3	−7.197	0.00	−0.18
	B_4	−7.210	−0.04	−0.18
	B_8	−7.214	0.00	−0.15
$C_2B_7H_{13}$	B_2	−7.542	−0.04	−0.12
	B_1	−7.596	0.05	0.00
	B_4	−7.601	0.13	0.05
	B_6	−7.613	−0.02	−0.07
	B_5	−7.632	0.13	0.07
	C_8	−11.259	−0.14	−0.01
$C_2B_9H_{12}^-$	B_{10}	−7.367	−0.01	−0.13
	B_{12}	−7.371	−0.01	−0.13
	B_2	−7.374	−0.04	−0.10
	B_3	−7.384	0.05	−0.09
	B_7	−7.399	0.02	−0.09
	B_8	−7.434	0.07	−0.04
	C_4	−11.091	−0.05	−0.05
$C_2B_{10}H_{13}^-$	B_7	−7.388	−0.02	−0.14
	B_{12}	−7.388	−0.01	−0.12
	B_4	−7.390	−0.01	−0.14
	B_8	−7.396	0.04	−0.08
	B_{10}	−7.420	0.03	−0.09
	B_3	−7.428	0.12	−0.01
	C_2	−11.080	−0.08	−0.08
	C_{13}	−11.105	0.02	0.03

[a] Units are atomic units (au). [b] Charges are in electrons (e).

Table III. Dipole Moments[a]

Molecule	PRDDO μ	Ab initio μ
B_8H_{12}	4.04	3.75
B_8H_{14}	3.88	
B_9H_{15}	3.95	3.70
$B_{10}H_{14}$	4.92	4.56
$C_2B_7H_{13}$	4.65	

[a] Dipole moments are in debye.

neutral, mononegative, and dinegative species using the relationship

$$\epsilon_i = b_0 + b_1 q_i$$

The statistical results are given in Table V. We also performed a multiple linear regression analysis using the expanded relationship

$$\epsilon_i = b_0 + b_1 q_i + b_2 Q$$

where Q is the net charge of the species in question. These results are also given in the table. The standard deviations of the estimates for ϵ_i range between 0.02 and 0.03 au in all cases. However, the correlation coefficients, r, are consistently larger when the *group* charges are employed, a result perhaps not unexpected since the inner shell eigenvalues are necessarily responsive to concentrations of charge lying at some distance from the parent nucleus.

In choosing one site over another for electrophilic or nucleophilic attack, we shall insist upon a difference in inner-shell eigenvalues of at least 0.02 au and a difference in atomic or group charges of at least 0.03 electrons. As expected from the statistical results presented above, the three indicators usually give rise to similar predictions. In particular the eigenvalues and the group charges yield identical predictions for the sites *most* susceptible to electrophilic and to nucleophilic attack. Of course, more detailed orbital control can lead to violations of these simple rules, as in 4,5-$C_2B_4H_8$.[27] Nevertheless, successful predictions have been obtained for other cases in which detailed experimental results are available for comparison, e.g., for $B_{10}H_{14}$.[26a,28] We await experimental verification for most of the following predictions, which indeed we offer in the hope and expectation that they will prove to be helpful in interpreting the experimental data as it becomes available. The instances cited below in which the reactivity indices differ provide another opportunity—that of eventually determining which set of indices best accommodates the experimental data.

In covalent processes, reactivity often correlates with, and appears to be controlled by, the highest occupied and lowest unoccupied molecular orbitals. Such a degree of specificity is probably not to be expected in ionic processes, but it stands to reason that reactivity should be affected principally by charge distributions occurring in readily perturbed molecular orbitals, i.e., in the few or several highest occupied orbitals. As in previous accounts,[26a,28] we therefore consider sums of atomic populations over successive numbers of n highest occupied molecular orbitals. The use of a step weighting function in this approach contrasts to the equal weights implicitly assigned in the indices based on gross electronic charge and might be expected to err in the opposite sense in comparison to a proper (but unknown) weighting scheme. In order for the sum predictions to agree with the experimental results for $B_{10}H_{14}$, it was found that n must be at least three.[26a] We here apply the sum analysis to the molecules in the B_8H_{12} family in order to compare the predictions so obtained with those based on total charges. We note that the problem of where to terminate the series becomes more difficult as the molecules become larger

Table IV. Overlap Population and Bond Distances for Boron Hydrides and Ions

Molecule	Bond	Bond length[a]	Overlap population	Molecule	Bond	Bond length[a]	Overlap population
B_8H_{14}	B_1-B_2	1.85	0.341	$B_{10}H_{13}^-$	B_1-B_2	1.75	0.491
	B_1-B_3	1.77	0.466		B_1-B_3	1.78	0.412
	B_1-B_4	1.71	0.445		B_1-B_4	1.79	0.410
	B_2-B_3	1.79	0.434		B_1-B_5	1.74	0.449
	B_2-B_8	1.76	0.459		B_1-B_9	1.78	0.433
	B_3-B_8	1.85	0.338		B_2-B_5	1.79	0.338
	B_3-B_4	1.87	0.344		B_2-B_7	1.77	0.469
	B_7-B_8	1.84	0.317		B_2-B_6	1.74	0.418
	B_4-B_5	1.83	0.283		B_2-B_3	1.77	0.424
	B_1-H_1	1.19	0.830		B_3-B_7	1.76	0.462
	B_2-H_2	1.19	0.827		B_3-B_8	1.73	0.508
	B_3-H_3	1.19	0.829		B_3-B_4	1.78	0.410
	B_4-H_4	1.19	0.812		B_4-B_8	1.76	0.429
	B_4-H_4'	1.19	0.745		B_4-B_{10}	1.70	0.531
	B_7-H_7	1.19	0.825		B_4-B_9	1.80	0.410
	B_4-H_9	1.33	0.377		B_7-B_8	2.04	0.328
	B_3-H_{10}	1.42	0.293		B_5-B_9	1.85	0.488
	B_8-H_{10}	1.29	0.500		B_5-B_6	1.65	0.831
	B_8-H_{11}	1.34	0.391		B_6-B_7	1.78	0.334
$B_8H_{13}^-$	B_1-B_7	1.88	0.297		B_8-B_{10}	1.78	0.345
	B_1-B_3	1.74	0.486		B_9-H_{10}	1.80	0.332
	B_1-B_4	1.71	0.478		B_1-H_1	1.19	0.832
	B_2-B_3	1.79	0.431		B_2-H_2	1.19	0.829
	B_2-B_8	1.79	0.484		B_3-H_3	1.19	0.834
	B_3-B_4	1.95	0.383		B_4-H_4	1.19	0.840
	B_3-B_8	1.74	0.317		B_5-H_5	1.19	0.818
	B_7-B_8	1.94	0.286		B_6-H_6	1.19	0.833
	B_4-B_5	1.86	0.424		B_7-H_7	1.19	0.829
	B_1-H_1	1.19	0.823		B_8-H_8	1.19	0.844
	B_2-H_2	1.19	0.813		B_9-H_9	1.19	0.840
	B_3-H_3	1.19	0.809		$B_{10}-H_{10}$	1.19	0.831
	B_4-H_4	1.19	0.791		B_6-H_{11}	1.30	0.328
	B_4-B_4'	1.19	0.795		B_7-H_{11}	1.19	0.497
	B_7-H_7	1.19	0.814		B_8-H_{12}	1.25	0.419
	B_3-H_9	1.33	0.356		$B_{10}-H_{12}$	1.29	0.396
	B_8-H_9	1.37	0.427		$B_{10}-H_{13}$	1.29	0.444
	B_8-H_{10}	1.35	0.387		$B_{10}-H_{13}$	1.28	0.371
$B_9H_{14}^-$	B_1-B_2	1.79	0.395	$B_{11}H_{13}^{2-}$	B_2-B_3	1.79	0.640
	B_1-B_3	1.78	0.404		B_2-B_{11}	1.76	0.421
	B_1-B_4	1.75	0.445		B_3-B_4	1.88	0.240
	B_1-B_5	1.74	0.466		B_3-B_{11}	1.79	0.402
	B_1-B_9	1.76	0.431		B_3-B_7	1.80	0.449
	B_2-B_5	1.77	0.430		B_4-B_5	1.84	0.498
	B_2-B_6	1.70	0.395		B_4-B_7	1.72	0.461
	B_4-B_9	1.87	0.356		B_7-B_8	1.79	0.411
	B_5-B_6	1.78	0.304		B_7-B_{12}	1.80	0.427
	B_5-B_9	1.95	0.377		B_7-B_{11}	1.80	0.427
	B_1-H_1	1.19	0.822		$B_{10}-B_{11}$	1.76	0.480
	B_2-H_2	1.19	0.817		$B_{11}-B_{12}$	1.82	0.418
	B_4-H_4	1.19	0.796		B_8-B_{12}	1.76	0.474
	B_4-H_4'	1.19	0.658		B_3-H_{13}	1.31	0.358
	B_5-H_5	1.19	0.823		B_4-H_{13}	1.24	0.487
	B_6-H_6	1.19	0.817		B_2-H_2	1.19	0.799
	B_8-H_8	1.19	0.803		B_3-H_3	1.19	0.772
	B_8-H_8'	1.19	0.784		B_4-H_4	1.19	0.812
	B_5-H_4	1.27	0.346		B_7-H_7	1.19	0.802
	B_6-H_{11}	1.20	0.479		B_8-H_8	1.19	0.805
					$B_{10}-H_{10}$	1.19	0.768
					$B_{12}-H_{12}$	1.19	0.804

[a] Bond lengths are in A.

and the symmetry decreases because there are then no well-defined gaps in the eigenvalue spectrum. In the discussions presented below, as many as the eight highest occupied orbitals have been included in the sums.

We turn now to a discussion of the reactivity predictions for electrophilic and nucleophilic processes starting with B_8H_{12} and its structural relatives. Based upon both eigenvalues and group charges, the orders of electrophilic attack for B_8H_{12} and B_8H_{14} (C_s) are predicted to be $B_2 > B_3 \sim B_1 \sim B_4 > B_7$ and $B_4 \sim B_2 > B_1 > B_7 \sim B_3$, respectively. The charge criteria slightly favor electrophilic attack at B_4 in B_8H_{14} (C_s) but we cannot confidently predict the preferred site for electrophilic substitution because the eigenvalue difference between B_4 and B_2 is so small. It is evident, however, that the addition of the extra terminal hydrogen on B_4 markedly increases the susceptibility of this site to electrophilic attack. In B_8H_{14} (C_s), B_3 is clearly singled out as the site for nucleophilic attack by the charge criteria but again, the difference in the eigenvalues between B_3 and B_7 is so small that we cannot distinguish between them. Based upon the eigenvalues and group charges, the order for electrophilic substitution in $B_8H_{13}^-$ should be $B_4 > B_2 \sim B_1 > B_3 > B_7$. Moreover, the terminal hydrogens bonded to B_4 and B_5 appear to be the most likely terminal hydrogens to be ab-

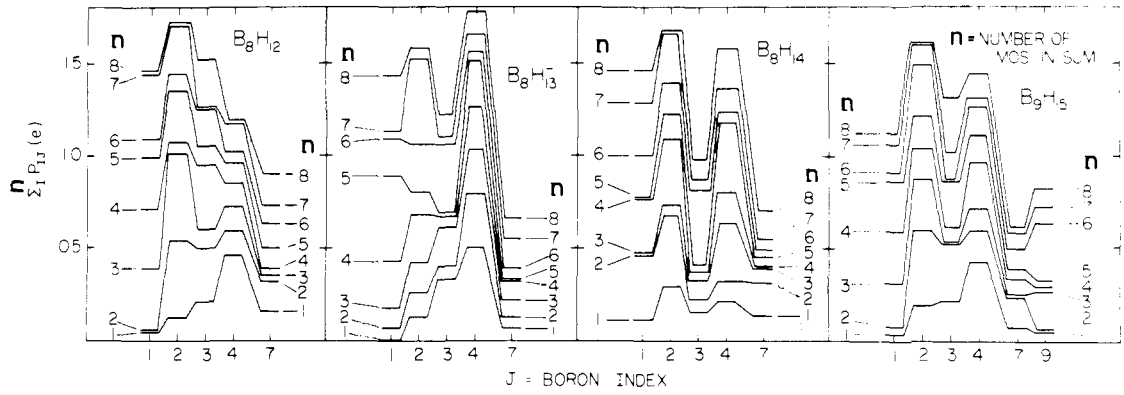

Figure 2. Sums of atomic populations over $n(n = 1\text{-}8)$ molecular orbitals for all of the unique centers for the molecules in the B_8H_{12} family, B_8H_{12}, B_8H_{14} (C_s), $B_8H_{13}^-$, and B_9H_{15}. Centers are numbered as in Figures 3-6.

Table V. Statistics for Linear Regression Analyses of Eigenvalue–Mulliken Charge Correlations[a]

A. $\epsilon_i = b_0 + b_1 q_i$

Q	b_0	b_1	σ[b]	r[c]	S_N[d]	Type of charge, q_i
0	−7.611	−0.464	0.017	0.884	28	Group
−1	−7.456	−0.542	0.022	0.855	33	Group
−2	−7.247	−0.307	0.021	0.723	11	Group
0	−7.597	−0.418	0.023	0.776	28	Atomic
−1	−7.390	−0.499	0.030	0.706	33	Atomic
−2	−7.198	−0.639	0.023	0.634	11	Atomic

B. $\epsilon_i = b_0 + b_1 q_i + b_2 Q$

b_0	b_1	b_2	σ[c]	r[c]	S_N[d]	Type of charge, q_i
−7.612	−0.474	−0.165	0.020	0.991	72	Group
−7.595	−0.459	−0.202	0.026	0.985	72	Atomic

[a] The linear regression analyses reported here were performed using subroutines from the Scientific Subroutine Package. [b] Standard deviation of estimate. [c] Correlation coefficient. [d] Sample size. Symmetrically related nuclei are included only once in the sampling.

stracted as hydride ions, in view of their well-developed negative charge (compare the atomic and group charges for B_4 in Table II) and the relatively small values for their BH_4 overlap populations (Table IV). These results would predict a facile conversion of $B_8H_{13}^-$ to B_8H_{12} via hydride loss. We only discuss hydride loss for terminal hydrogens as it is difficult to compare bridge and terminal hydrogens and because bridge hydrogens are often lost as protons ($B_{10}H_{14} \rightarrow B_{10}H_{13}^- + H^+$). We note here that atomic charges may be less appropriate than the group charges for predicting the reactivity of negative ions toward electrophiles because much of the net ionic charge is carried by the terminal hydrogens. For B_9H_{15}, we predict B_2 to be most susceptible to electrophilic attack and B_7 to be most susceptible to nucleophilic attack. Addition of the BH_3 group also promotes the susceptibility of B_4 to electrophilic attack in comparison to its reactivity in B_8H_{12}. The most marked features in this series are the increasing susceptibility of B_4 to electrophilic attack with increasing substitution in that region and the emergence of B_7 as the generally preferred site for nucleophilic attack.

The sums of populations over the several highest occupied molecular orbitals are depicted in Figure 2 for the B_8H_{12} family. Unfortunately, reactivity predictions based upon populations of the HOMO correlate poorly with the reactivity order predicted by charges or eigenvalues. For example, in opposition to the charge or eigenvalue predictions, the HOMO populations clearly predict B_4 as the preferred site for electrophilic attack in B_8H_{12} and B_9H_{15}. For B_8H_{14} (C_s), the HOMO correlates well with charges or eigenvalues in predicting the site for electrophilic attack but does very poorly in predicting the site for nucleophilic attack. After summing the populations over the first four or five orbitals, the sum predictions agree reasonably well with those based on total charge distributions and eigenvalues. However, exceptions still occur. For example, in B_8H_{14} (C_s) B_7 is favored over B_3 as the site for nucleophilic attack by the sum criteria where the charge criteria definitely favored B_3 as the preferred site. Furthermore, using the population sums, inversions in the predicted reactivity order still occur between consecutive sums even for $n = 4$. Since there is no well-defined energy gap in the eigenvalue spectrum, the choice for an upper limit for n is somewhat arbitrary. We have applied the sum analysis to the remaining molecules discussed below and have found that the sums with $n \geq 4$ usually predict the same sites of preferential electrophilic and nucleophilic attack as do the charge and eigenvalue criteria.

For the structural relatives of $B_{10}H_{14}$, $B_9H_{14}^-$, and $B_{10}H_{13}^-$, the eigenvalues and group charges allow us to predict the most likely sites for electrophilic and nucleophilic substitution, but not the detailed order. For $B_9H_{14}^-$, these sites are B_4 and B_5 (or B_6), respectively, and are B_5 and B_{10} for $B_{10}H_{13}^-$. For the parent $B_{10}H_{14}$ molecule, the order for electrophilic attack based upon eigenvalues and charges is $B_2 \sim B_1 > B_5 > B_6$, in agreement with the SCF results and experiment.[26,28] Among the terminal hydrogens in $B_{10}H_{13}^-$, H_5 has the most highly developed negative charge and has the smallest B-H overlap population (Table IV). We therefore predict that this hydrogen will be the most readily abstracted as a hydride ion among terminal hydrogens. Similar considerations point to H_4' in $B_9H_{14}^-$ as the most easily abstracted terminal hydride ion. In $B_{10}H_{14}^{2-}$, electrophilic attack seems clearly preferred at B_6, with nucleophilic attack, if feasible, occurring preferentially at B_2 or, possibly, B_5.

For $B_{11}H_{13}^{2-}$, the preferred site for electrophilic attack based upon eigenvalues and group charges is B_2, while preferential nucleophilic attack would most likely take place at B_4 or B_8, but might occur at any site except B_2. Electrophilic attack at boron should take place preferentially at B_2, and nucleophilic attack at B_5, in $C_2B_7H_{13}$, while in $C_2B_9H_{12}^-$, only B_8 is an unlikely site for electrophilic attack. In $C_2B_{10}H_{13}^-$, electrophilic attack at boron might occur preferentially at any site except B_3.

In polyhedral carboranes, $C_2B_{n-2}H_n$, the reactivity indices suggest[29,30] the following rule: nucleophilic attack should occur principally at boron(s) adjacent to carbon and,

conversely, distant borons should be the most susceptible to electrophilic attack. However, the results for the nido carboranes studied here suggest that this rule should be based only upon proximity to CH groups, and not upon proximity to CH_2 groups. Thus in agreement with the rule, B_8, which is adjacent to both C_4 and C_5, is predicted (on the basis of charges and eigenvalues) to be the preferred site for nucleophilic attack (if feasible) in $C_2B_9H_{12}^-$ (Figure 15) and B_3, which is adjacent to C_2, is the indicated nucleophilic site in $C_2B_{10}H_{13}^-$ (Figure 16). No predictions based on proximity to carbon should be made for $C_2B_7H_{13}$ (Figure 12), which has only CH_2 groups, since the indices suggest that B_5 is the preferred site for nucleophilic attack and that B_2 is the preferred site for electrophilic attack, as we have seen.

In Table III we list the dipole moments for B_8H_{12}, B_8H_{14} (C_s), B_9H_{15}, $B_{10}H_{14}$, and $C_2B_7H_{13}$ calculated from the PRDDO wave functions. Clearly these agree quite well with those from the ab initio SCF calculations.

Overlap populations for boron hydrides calculated from ab initio wave functions fall roughly within the ranges:[23] B-B, 0.350-0.500; B-H_B, 0.380-0.420; B-H_t, 0.750-0.830, as do the PRDDO values given in Table IV. We note that the overlap populations for the boron hydrides and boron hydride ions discussed in ref 23 all fell into the same relative order within a given molecule as did the ab initio values, further illustrating the closeness with which PRDDO method reproduces the ab initio charge distributions. We therefore feel that the quantities listed in Tables II, III, and IV are also likely to be in excellent agreement with those that would be given by ab initio calculations employing the same basis sets.

Boys Localizations. After giving a brief account of the Boys method, we shall turn to a discussion of structural interrelationships in the several molecules and ions considered here as elucidated from the localization results. Following Boys,[1,3] we perform a unitary transformation on the occupied canonical molecular orbitals (CMO's) which maximizes the sum of squares, D, of displacements of the orbital centroids from the arbitrarily defined origin of the molecular coordinate system. The quantity D is defined as

$$D = \sum_{i=1}^{n} \langle \phi_i | \bar{r} | \phi_i \rangle \cdot \langle \phi_i | \bar{r} | \phi_i \rangle \qquad (1)$$

where the summation extends over all n doubly occupied molecular orbitals. Successive two-orbital transformations as suggested by Edmiston and Ruedenberg (ER procedure), each of which must either increase D or leave it unchanged, are applied. Each complete iteration cycle of the procedure consists of $n(n-1)/2$ such transformations of orbital pairs and is characterized by the unitary transformation matrix, **T**, which carried the CMO's into the LMO's of that cycle. Convergence is operationally defined by the condition that no element of **T** changes by more than 10^{-4} in the course of a complete cycle of the two-orbital transformations. The localized orbitals for B_8H_{12}, B_8H_{14} (C_s), $B_8H_{13}^-$, B_9H_{15}, $B_{10}H_{14}$, $B_{10}H_{13}^-$, $B_9H_{14}^-$, $C_2B_7H_{13}$, $B_{10}H_{14}^{2-}$, $B_{11}H_{13}^{2-}$, $C_2B_9H_{12}^-$, and $C_2B_{10}H_{13}^-$ are illustrated in Figures 3-16. In each case, the root mean square change in **T** had fallen to at least 10^{-3}, but usually not to less than 10^{-4}, after 10-15 iteration cycles, indicating substantial but frequently incomplete convergence. Slow convergence typically occurs when the localization is relatively insensitive to closely coupled changes involving three or more LMO's, a situation that is not well handled by the two-orbital transformation procedure.[1]

For some of the more difficult cases, we therefore have applied an alternative, multiorbital, transformation to the partially converged orbitals given by the two-orbital transformations. Designated the eigenvector procedure,[1] this transformation employs, normally, the eigenvector corresponding to the most positive eigenvalue of the matrix of second derivatives of D with respect to orthonormal variations in the localized orbitals. This eigenvector "points" in the direction on the sum-of-squares (SOS) surface of most positive curvature and expresses the desired coupled changes in the least well determined localized orbitals. This and other aspects of the localization procedure are fully described in ref 1. The sequence for $B_9H_{14}^-$ is typical: ten iteration cycles of $n(n-1)/2$ two-orbital transformations, one eigenvector transformation, and four more iteration cycles. Since each eigenvector cycle is equivalent in CPU time to about five iteration cycles, this sequence requires approximately the same time as would 19 iteration cycles. This should be compared to the 24 iteration cycles required in this case when the 2×2 procedure is used alone.

Table VI. Least Well Determined LMO's

Molecule	Highest second[a] derivative eigenvalue	Principally involved LMO's
B_8H_{12}[b]	−7.60	$B_2-B_7-B_8$, B_2-B_6, B_2-B_3
B_8H_{14} (C_s)	−4.28	$B_2-B_3-B_8$, $B_2-B_6-B_7$, B_1-B_2
$B_8H_{13}^-$	−2.02	$B_2-B_7-B_8$, B_2-B_3, B_2-B_6
B_9H_{15}	−4.05	$B_2-B_7-B_8$, $B_1-B_2-B_3$, $B_1-B_2-B_6$
$B_{10}H_{14}$[b]	−1.61	$B_2-B_6-B_7$, $B_4-B_8-B_{10}$, $B_4-B_9-B_{10}$, $B_2-B_5-B_6$, $B_1-B_3-B_4$, $B_1-B_2-B_3$
$B_{10}H_{13}^-$	−2.40	$B_4-B_8-B_{10}$, $B_1-B_3-B_4$, B_4-B_9
$B_9H_{14}^-$	−2.88	$B_1-B_2-B_3$, $B_2-B_5-B_6$, $B_2-B_6-B_7$
$C_2B_7H_{13}$[b]	−7.42	$B_1-B_2-B_5$, $B_2-B_3-B_7$, B_2-B_6
$B_{10}H_{14}^{2-}$	−6.10	$B_3-B_4-B_8$, $B_2-B_3-B_7$, B_1-B_3, $B_1-B_2-B_5$, $B_1-B_4-B_{10}$
$B_{11}H_{13}^{2-}$	−4.70	$B_8-B_9-B_{12}$, $B_7-B_8-B_{12}$, $B_{10}-B_{11}-B_{12}$
$C_2B_9H_{12}^-$	−5.12	B_2-H', $B_2-B_6-B_{10}$, $B_2-B_3-B_{11}$
$C_2B_{10}H_{13}^-$	−3.60	C_2-B_6, C_2-B_3, $C_2-B_{10}-B_{11}$

[a] Unless noted, inner shells were not included in the second derivative test. [b] Inner shells included in the second derivative test.

A key analysis of the resultant LMO's is provided by a limited second derivative test (LSDT),[1] which yields a curvature analysis of the LMO hypersurface. For purposes of efficiency the LSDT is performed in a subspace of the full orbital-pair space. The details of implementing the LSDT have been described elsewhere,[1] and it will suffice to say here that the procedure consists of constructing a second-derivative matrix D_2, diagonalizing D_2, and examining the resultant eigenvalues and eigenvectors. If all eigenvalues of D_2 are negative, D_2 is negative definite and, if convergence of T has been attained, a relative maximum on the "sum of squares" surface has been reached. If one or more eigenvalues of D_2 are positive at convergence, the localization has reached a saddle point. Finally, the presence of one or more small or nearly zero eigenvalues indicates that the localization is insensitive to certain couplings of orbitals as specified by the eigenvectors belonging to the nearly vanishing eigenvalues. The occurrence of flat maxima is not peculiar to the Boys sum of squares (SOS) criterion. Thus, the localization of B_5H_9[31] yields flat maxima on both the Boys SOS surface and the ER self-energy surface.[1] In addition, saddle point structures have been observed on both the SOS and self-energy surfaces for 1,2-$C_2B_4H_6$.[1] We cite in Table VI the most positive LSDT eigenvalue for each molecule and list the LMO's that are least well determined as specified by the corresponding eigenvector. These LMO's are indeed found to be the least transferable, as judged by comparisons of LMO structures for similar molecules (see below).

Each localization was repeated as many as ten times with different starting sets of MO's generated by random unitary transformations of the initial CMO's. This procedure al-

Table VII. Topologically Allowed Structures for the B_8H_{12}-Like Molecules

Molecule	Structure	B–B	Bonds[a]	
B_8H_{12}	A1	3–4	5–6	(1)
	A2	3–4	2–6	(2)
	A3	3–4	2–8	(2)
B_8H_{14} (C_s)	B1	2–3		(2)
	B2	2–8		(2)
	B3	1–2		(1)
$B_8H_{13}^-$	C1	2–3	4–5	(2)
	C2	2–3	5–6	(2)
	C3	2–8	5–6	(2)
	C4	2–8	4–5	(2)
	C5	1–2	4–5	(1)
	C6	3–4	5–6	(1)
B_9H_{15}	D1	1–2	4–5	(1)
	D2	2–3	4–5	(2)
	D3	3–4	2–6	(2)
	D4	3–4	2–8	(2)
	D5	3–4	5–6	(1)
	D6	4–5	2–8	(2)

[a] Only B–B bonds are given in the topological tables because the three-center bonds are then uniquely determined aside from satisfying the molecular symmetry. The numbers in parentheses give the number of symmetrically equivalent structures with the indicated topology.

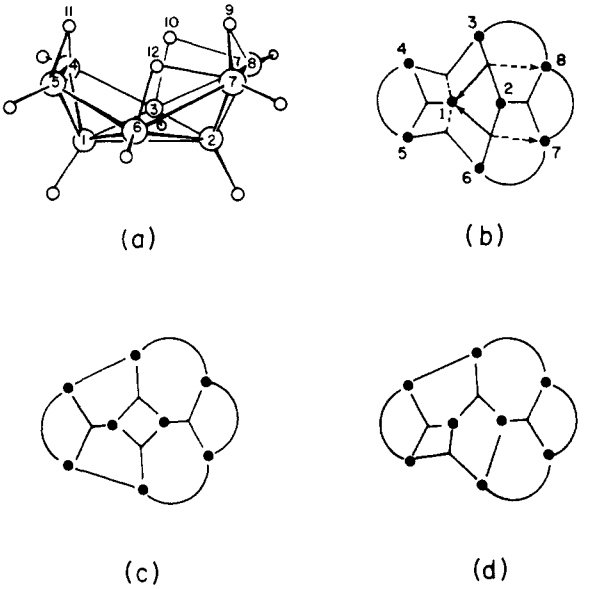

Figure 3. Geometry, localized valence structure, and topologically allowed valence structures for B_8H_{12}: (a) geometry of B_8H_{12}, symmetry C_s; (b) localized valence structure for B_8H_{12}; (c) and (d) topologically allowed valence structures. Structures c and d are structures A1 and A2 of Table VI, respectively.

lowed a test of the uniqueness of the localizations. Except as required by symmetry, no multiple maxima were found.

Results for Localized Orbitals

In this section we discuss and analyze the localized orbitals for each of the molecules and ions. In order to describe the electron density pictorially, the following conventions have been observed in drawing the representations of the localized orbitals which appear in Figures 2–15. (a) For each LMO, only centers having populations of at least 0.15 e are included in the pictorial representation. (b) Centers with populations in the range 0.15–0.25 e are connected with a dashed arrow (⇢). (c) Centers with populations in the range 0.25–0.35 e are connected with a solid arrow (→). (d) Centers with populations in the range 0.35–0.50 e are connected with a dashed line (- - - -). (e) All other centers in a given LMO (dominant centers) are connected with solid lines.

B_8H_{12}. The geometry of B_8H_{12} is depicted in Figure 3a. The localized valence structure for B_8H_{12} (Figure 3b) is quite interesting because B_1 participates in five framework bonds as well as a terminal BH bond. Usually no more than four framework bonds to any one boron atom are observed.[26b] The framework bonds to B_1 show definite asymmetry, the 4–5–1 bond being the only B–B–B bond having nearly equal populations on each boron (0.70, 0.70, 0.60 e). The equivalent 4–3–1 and 5–6–1 bonds have populations of 0.77, 0.82, and 0.38 e, showing a more typical fractional bonding to B_1. The 3–2–1 and 6–2–1 bonds have populations of only 0.31 e on B_1 and display substantial contributions (0.20 e) from B_8 and B_7. From Figure 3 we see that the localized structure (3b) is evidently a combination of the topologically allowed (TA) structures 3c and 3d. A list of topological structures for B_8H_{12} is given in Table VII. (Structures c and d of Figure 3 are A1 and A2 in Table VII.)

The localized orbital method and the topological approach complement each other nicely. Topological theory is based upon simple rules for connecting atoms by two- and three-center bonds and provides useful simplified valence structures for the boranes. The localized orbital approach has proved helpful in suggesting modifications to the topological theory.[32] In the case of B_8H_{12} and other molecules in which fractional bonding is present, the pattern of bonding expressed by the localized valence structure generally corresponds to that expected for a weighted sum of several TA structures.

B_8H_{14}. Lipscomb originally proposed a C_s structure[33] for B_8H_{14} while Dobson and Schaeffer[34] proposed a C_{2v} structure based on the ^{11}B NMR results. In order to determine a reasonable structure for B_8H_{14}, a series of geometry optimizations was carried out for the C_s and C_{2v} structures. The C_s geometry was constructed by adding a bridge hydrogen between B_4 and B_5 of $B_8H_{13}^-$ and the position of the bridge hydrogen was optimized. Another initial C_s geometry was obtained by adding terminal hydrogens to B_4 and B_5 of B_8H_{12}, and then optimizing the positions of the bridge hydrogens H_{10} and H_{12} (Figure 3). The two structures were linked by a linear synchronous transit (lst) path[35] yielding an intermediate geometry of lower energy. The C_{2v} geometry was obtained by reflecting the coordinates of the half of B_8H_{12} with three bridge hydrogens through the plane containing B_3 and B_6 and their terminal hydrogens and then by optimizing the position of the four symmetry related bridge hydrogens. This same procedure was used starting from the $B_8H_{13}^-$ coordinates. The two C_{2v} geometries were connected by an lst path again yielding a lower energy structure. The best C_s and C_{2v} structures obtained from the lst path results were connected by an lst path which yielded an intermediate structure at a lower energy than either end point with no energy barrier present. The final structure showed C_s character and had moved 40% of the way along the lst path starting from the C_s structure. The final structure for which we present results was more stable than the C_{2v} structure by 22 kcal/mol. However, as the geometries have not been fully optimized and the energy difference is small, we cannot predict with certainty the structure of the system. As the energy surface for B_8H_{14} is quite flat, tautomeric hydrogen shifts between the BH_2 and partial or complete BHB groups may be occurring. Perhaps these shifts could account for the ^{11}B NMR spectrum, which shows an unsymmetrical triplet for the fourfold set of borons.[34b] The new terminal hydrogens on B_4 and B_5 in the optimized C_s structure show a small amount of bonding to B_3 and B_6 of

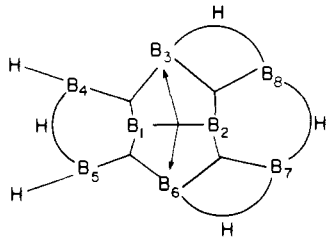

B_8H_{14}

Figure 4. The localized valence structure for B_8H_{14} (C_s). Extra terminal hydrogens are found on B_4 and B_5. For the C_{2v} structure, the 6-1-5 and 3-1-4 bonds become like the 6-2-7 and 3-2-8 bonds of the C_s structure.

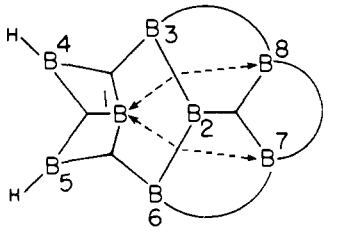

$B_8H_{13}^-$

Figure 5. The localized valence structure for $B_8H_{13}^-$.

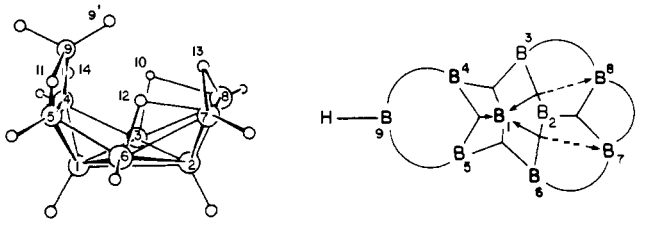

B_9H_{15}

Figure 6. The geometry (a) and localized valence structure (b) of B_9H_{15}, symmetry C_s.

0.07 e and this small amount of bonding could also account for the ^{11}B NMR of B_8H_{14}. A similar result is found in B_5H_{11} where the apical BH_2 group is not seen as a BH_2 group in the ^{11}B NMR due to the unique hydrogen showing a small amount of bridging character (0.10 e) to other borons.[36]

The localized valence structure of B_8H_{14} (C_s) (Figure 4) has simple two- and three-center bonds and corresponds nicely to the 4412 topology originally proposed by Lipscomb.[33] The only fractional bonding involves contributions of 0.29 e to the 1-2 bond from B_3 and B_6. The framework bonds do not have symmetric charge distributions. Rather, the bonds to B_3 and B_6 show less density at these centers (0.43 e from 8-2-3 and 7-2-6 and 0.58 e from 4-1-3 and 5-1-6). The two symmetry related bridge bonds are nonsymmetric, 0.40 e on B_3 and B_6 and 0.64 e on B_8 and B_7, as required by geometry. The five TA structures for (4412) B_8H_{14} are listed in Table VII. The localized structure corresponds to the TA structure which has a single bond between B_1 and B_2. The addition of two terminal hydrogens has changed the environment at B_4 and B_5 in such a way that each boron participates in only one three-center B-B-B bond. Elimination of the 1-4-5 bond of B_8H_{12} also transforms the least well determined LMO's of B_8H_{12} (i.e., 2-3, 2-6, and 2-7-8) into the 1-2, 2-3-8, and 2-6-8 bond LMO's of B_8H_{14} yielding one two-center and two three-center framework orbitals, and hence, a normal topology.

In going to the C_{2v} structure of B_8H_{14} from the C_s structure, the B_4-H_4' and B_5-H_5' terminal hydrogens become very asymmetric bridge hydrogens while the bridge hydrogens between B_3 and B_8 and B_6 and B_7 become more asymmetrical. The final boron populations for the bridge hydrogen bonds are 0.25 e on the central borons (B_3 and B_6) and 0.75 e on the end borons (B_4, B_5, B_7, and B_8). Thus, little change is found in the LMO's in going from the C_s to the C_{2v} structure. The only change is that the 3-1-4 and 6-1-5 bonds lose density at B_3 and B_6 and the 3-2-8 and 6-2-7 bonds gain in density at these borons giving four equivalent framework orbitals with 0.73 e on the end atoms (B_4, B_5, B_7, and B_8), 0.73 e on the apical atoms (B_1 and B_2), and 0.48 e on the central atoms (B_3 and B_6). The C_{2v} structure is a resonance hybrid of two topologically disallowed 6230 structures.[28] The LMO's for the C_{2v} structure bear a strong resemblance to the five framework orbitals at the bottom of the $B_{10}H_{14}^{2-}$ basket (Figure 13).

$B_8H_{13}^-$. The localized structure for $B_8H_{13}^-$ (Figure 5) is very much like that of B_8H_{12} with minor, though definite, differences in the relative populations in the framework orbitals. Chemically, $B_8H_{13}^-$ can be envisioned as the result of attack of a hydride ion on B_8H_{12} at B_4 or B_5, with concomitant conversion of the B_4-H_b-B_5 bond into a B-H_t bond, or of loss of a proton from the B_4-H_b-B_5 bridge of B_8H_{14} (C_s). Indeed, the differences in the LMO structures of B_8H_{12}, $B_8H_{13}^-$, and B_8H_{14} can be rationalized in terms of the number of electrons B_4 and B_5 can formally donate to the boron framework. In a neutral boron hydride, each boron contributes three valence electrons. Formally, B-H_t bonds each require one electron from boron, while BH_bB bonds incorporate 0.5 e from each boron. In B_8H_{12}, therefore, B_4 and B_5 each donate 1.5 e to the framework, while each donates 0.5 in B_8H_{14}. For the purposes of this argument, we assume that the negative charge in $B_8H_{13}^-$ is shared by B_4 and B_5 so that each donates 1.5 e to the framework, as in B_8H_{12}. As a result, the LMO valence structures of B_8H_{12} and $B_8H_{13}^-$ are very similar. In contrast, the addition of two terminal hydrogens to B_4 and B_5 in B_8H_{12} or of a proton to $B_8H_{13}^-$ to form B_8H_{14} removes two electrons from the framework, with the result that the 1-4-5 bond of B_8H_{12} and B_8H_{13} is not present in B_8H_{14}. The remaining orbitals then adjust to minimize the electron deficiency in the B_1, B_4, B_5 region of the B_8H_{14} molecule. We note that the orbitals that react most dramatically to this perturbation are those that are least well determined as judged by the second derivative test results (Table VI).

The localized structure for $B_8H_{13}^-$ also corresponds to a combination of TA structures, specifically, of structures C4, C5, and C6 in Table VII. We note that if the localized structure did not have the fractional bonding, it would have the correct number of bonds for a TA structure (styx = 3422) but would *not* be topologically allowed because B_1 and B_2 would be nonbonded nearest neighbors.

B_9H_{15}. The molecule B_9H_{15} (Figure 6) can be obtained from B_8H_{12} by removal of bridge hydrogen H_{11} and addition of a H-(BH_2)-H group to form bridges with both B_4 and B_5. As in the comparison of B_8H_{14} and $B_8H_{13}^-$ with B_8H_{12}, the boron framework bonding depends to a great extent on the number of electrons contributed to the framework by B_4 and B_5. As each participates in a B-H_b-B and a B-H_t bond in B_9H_{15}, each again contributes 1.5 e to the framework and the framework bonding (Figure 6) is very nearly the same as in B_8H_{12} (Figure 3b). Consequently, five of the ten TA structures (Table VII) are the same as for B_8H_{12} and the structures that dominate in B_8H_{12} (Table

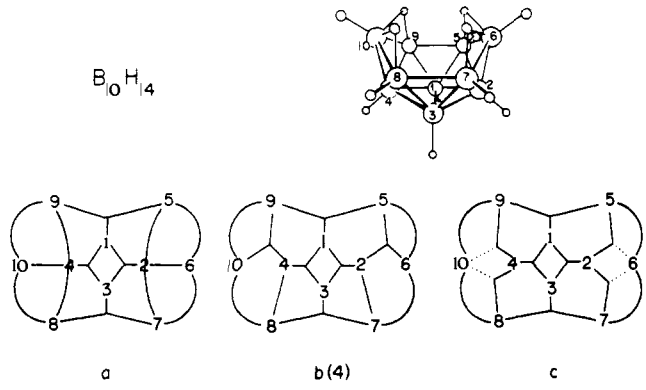

Figure 7. Topologically allowed (a and b) and localized (c) valence structures for $B_{10}H_{14}$. The geometry of $B_{10}H_{14}$ is illustrated in the upper right hand corner of the figure.

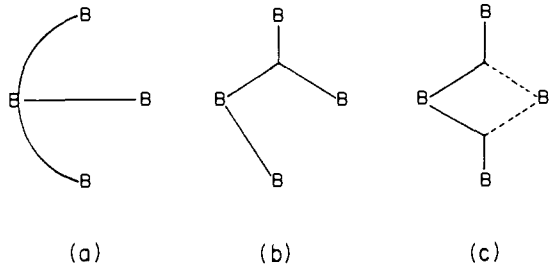

Figure 8. Possible bonding patterns for four boron atoms with four valence electrons available for framework bonding. The open three-center B-B-B bonds of (a) have never been observed in an LMO structure. The symmetric pattern (c) is the favored pattern.

VII, A1, A2) correspond to those TA structures of B_9H_{15} (D3 and D5) which contribute strongly to the localized structure (Figure 6b). However, TA structure D2 (Table VII), which has two center 4-5 and 2-3 (or 2-6) interactions, apparently also contributes to the weighted sum of TA structures that correspond to the localized structure of B_9H_{15}. Thus, the 4-5-1 bond in B_8H_{12} becomes more of a B4-B5 two-center bond in B_9H_{15} with donation (0.28 e) to B_1, and the 4-3-1 and 5-6-1 bonds in B_9H_{15} then react by donating a larger proportion of the two electrons allocated to them to B_1 than do the same bonds in B_8H_{12}.

$B_{10}H_{14}$. Decaborane(14) (Figure 7) has been the subject of ab initio SCF investigations[26a] as well as Edmiston–Ruedenberg localized orbital studies employing INDO wave functions.[37] The INDO localized valence structure and our localized structure (Figure 7c) are identical with the localized structure predicted by Lipscomb.[4] Open B-B-B bonds have not been observed in either Boys or ER localizations. Each method instead prefers symmetric fractional bonds rather than the combination of a single B-B bond and an open three-center B-B-B bond shown in Figure 7a for the open three-center TA structure for $B_{10}H_{14}$. Figure 7b gives one of the four central three-center TA structures. The localized structure (Figure 7c) is then correctly predicted from either 7a or 7b using the relationships in Figure 8. We note that the $B_{10}H_{14}$ framework LMO's are among the least well determined of any molecule studied in this paper (Table V). Thus, considerable changes in the LMO's can be expected when this system is structurally perturbed.

$B_{10}H_{13}^-$. The ion $B_{10}H_{13}^-$ (3630 topology) has the same boron framework as $B_{10}H_{14}$, from which it is obtainable by removal of the bridge hydrogen between B_5 and B_6 as a proton. The fractional bonding here (Figure 9) differs principally from that in $B_{10}H_{14}$ in that the 2-5-6 bond becomes a 1-2-5 bond and the 4-10-9 bond becomes a highly delocalized 4-9 single bond. In addition, the 1-5-9, 1-4-3, and 1-2-3 bonds become fractional to B_1. Thus, the stress placed on the LMO's by adding a pair of electrons to the framework in the form of the 5-6 bond modifies the remaining weakly determined framework LMO's in the manner needed to avoid the newly developed region of electron density.

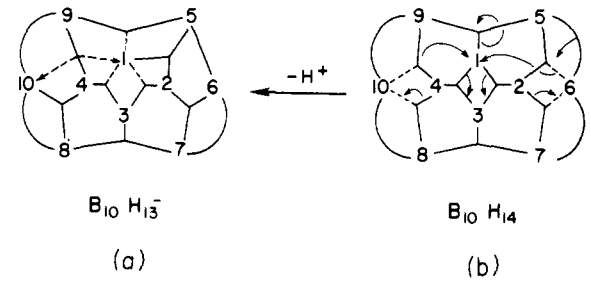

Figure 9. The localized valence structure of $B_{10}H_{13}^-$: (a) LMO structure for $B_{10}H_{13}^-$; (b) LMO structure for $B_{10}H_{14}$. The arrows show how the $B_{10}H_{14}$ bonds rearrange to the $B_{10}H_{13}^-$ bonds when a bridge hydrogen is removed from between B_5 and B_6 of $B_{10}H_{14}$.

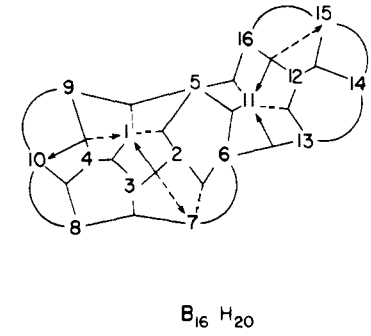

Figure 10. Localized valence structure for $B_{16}H_{20}$.

In a previous communication,[38] we analyzed the LMO's for $B_{16}H_{20}$ (Figure 10) and noted the similarity of the framework bonding of the B_{10} fragment in $B_{16}H_{20}$ to that in $B_{10}H_{14}$. It was shown that the difference in charge distributions for the B_{10} fragments in $B_{16}H_{20}$ and $B_{10}H_{14}$ correlates well with the difference in bonding.[30] Thus, B_1 is more positive in $B_{16}H_{20}$ than in $B_{10}H_{14}$, and B_2, B_3, and B_4 become more negative, as measured by Mulliken charges. The fractional bonding at B_1 can be viewed as a donation from electron-rich to electron-poor regions.[38] Similarly, the fractional center, B_7, has a more positive Mulliken charge in $B_{16}H_{20}$ than in $B_{10}H_{14}$, consistent with the observation that fractional centers tend to be relatively positive.

Comparison of Figures 9 and 10 shows that the LMO's in the B_{10} fragment of $B_{16}H_{20}$ correspond more nearly to those of $B_{10}H_{13}^-$ than to those of $B_{10}H_{14}$. Evidently the perturbation placed on the $B_{10}H_{14}$ system by fusion of the B_8 fragment is similar to that resulting from the removal of a bridge hydrogen (as H^+) from $B_{10}H_{14}$. The perturbations are indeed similar topologically, in that removal of H^+ from $B_{10}H_{14}$ produces a 5-6 bond while fusion of the B_8 fragment introduces a 5-6-11 bond to which B_{11} contributes only 0.53 e. Furthermore, the loss of the terminal hydrogens on B_5 and B_6 is compensated by formation of the 6-13-11 and 5-16-11 bonds, in which the donation to B_{11} is small (~0.3 e for each bond).

$B_9H_{14}^-$. Lipscomb[39] first suggested that $B_9H_{14}^-$ might have a 2613 topology instead of the 5421 topology of the $B_9H_{14}L$ (L is a covalent ligand) and B_9H_{15}. Subsequently,

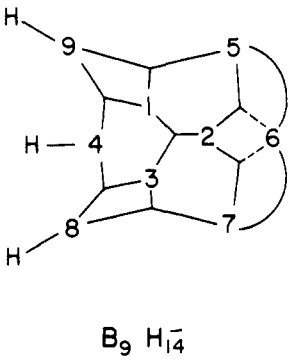

Figure 11. Localized valence structure for $B_9H_{14}^-$.

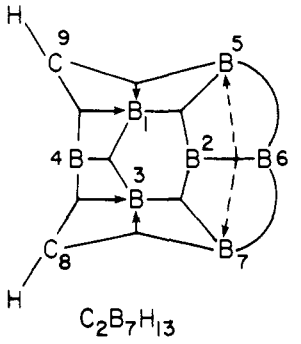

Figure 12. Localized valence structure for $C_2B_7H_{13}$.

this prediction was borne out by X-ray diffraction studies[12] of B_9H_{14} in the form of the cesium salt. The localized valence structure (Figure 11) exhibits the C_s symmetry of the ion. Excluding the bonds to B_4, the framework bonding is formally identical with that in $B_{10}H_{14}$ (Figure 7c). As B_4 has two terminal hydrogens, it can participate in at most two normal framework bonds. Hence, the 4-1-3 bond is lost, and the 4-10-9 and 4-8-9 bonds of $B_{10}H_{14}$ are substantially modified. Consequently, the only fractional bonding is at B_6.

$C_2B_7H_{13}$. The LMO's for $C_2B_7H_{13}$, which is isoelectronic with $B_9H_{14}^-$, again exhibit the C_s point symmetry of the molecule (Figure 12) but are quite different from those of $B_9H_{14}^-$. The major reason for the difference is the extra electron pair available for framework bonding in $C_2B_7H_{13}$ because of the presence of the carbon atoms at positions 8 and 9 and the single terminal hydrogen on B_4. Thus, B_4 now donates 2.0 e to the framework and can participate in three normal framework bonds. Atoms B_1 and B_3 are fractional centers which have two normal and two fractional bonds (contributions to B_1 are 0.26 e from the 9-5-1 bond and 0.29 e from the 9-4-1 bond). Also noteworthy is the presence of the delocalized 2-6 single bond. The unsymmetrical hydrogen bridges have populations of 0.61 e on B_6 and 0.41 e on B_5 and B_7, as expected from the molecular geometry.

The framework LMO's of $C_2B_7H_{13}$ can be formally constructed from those of $B_9H_{14}^-$ by considering the effect of exposing a pair of electrons at B_4 by removal of a proton to yield $B_9H_{13}^{2-}$. This electron pair would be expected to form the 4-1-3 bond present in $B_{10}H_{14}$ and to force a corresponding rearrangement of the remaining framework LMO's. Relaxation of charge density away from the 1-3-4 region might cause the 4-1-9, 5-1-9, 4-3-8, and 7-3-8 bonds to become fractional to B_1 and B_3, but the most marked changes would be expected in the least well determined LMO's (i.e., 1-2-3, 2-5-6, and 2-6-7). The optimal combination of these $B_9H_{14}^-$-like LMO's under the influence of the extra electron pair is apparently reflected in the formulation of the 2-6, 1-2-5, and 3-2-7 bonds. To test this supposition, we removed a proton from B_4 of $B_9H_{14}^-$ to give the hypothetical $B_9H_{13}^{2-}$ ion. The resulting LMO's were qualitatively the same as those of $C_2B_7H_{13}$. We also anticipate that protonation of B_4 to form $C_2B_7H_{14}^+$ would most likely result in the $B_9H_{14}^-$ bonding scheme, if this positive ion could be persuaded to retain the added proton.

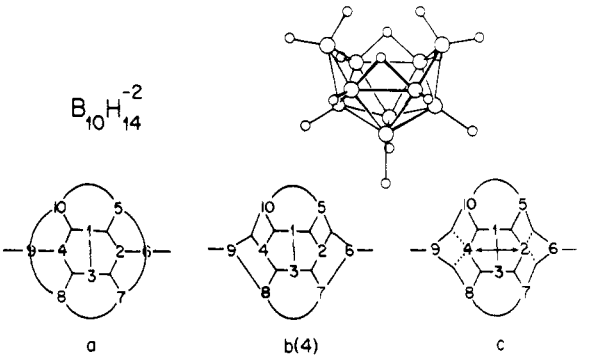

Figure 13. Topologically allowed (a and b) and localized valence structures (c) for $B_{10}H_{14}^{2-}$. The geometry of $B_{10}H_{14}^{2-}$ is illustrated in the upper right hand corner of the figure.

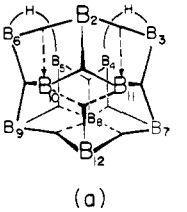

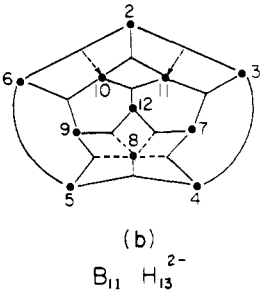

Figure 14. Localized valence structure for $B_{11}H_{13}^{2-}$ (a). The planar projection of the LMO's is shown in (b) to illustrate the symmetry of the localized orbitals and for comparison purposes.

$B_{10}H_{14}^{2-}$. Kendall and Lipscomb[13] employed the configurations in Figure 13a and 13b to predict basically the LMO structure shown in Figure 13c. Our detailed results differ from their prediction only in the appreciable donation to fractional centers B_2 and B_4 from the 1-3 bond (Figure 12e).

$B_{11}H_{13}^{2-}$. The $B_{11}H_{13}^{2-}$ ion is described as an icosahedron missing a vertex. The LMO's exhibit the C_s symmetry of the molecule (Figure 14). The bonding can perhaps best be described by showing how the two rings of five borons and the vertex are connected. Excepting the essentially two-center 2-6 and 2-3 bonds, three three-center B-B-B bonds connect the apex, B_{12}, to the lower five-membered ring and six three-center bonds, five of which have two centers in the lower ring, join the two five-member rings. The LMO (5-8-4) which has two centers in the upper ring shows only fractional bonding to the lower ring. The only fractional

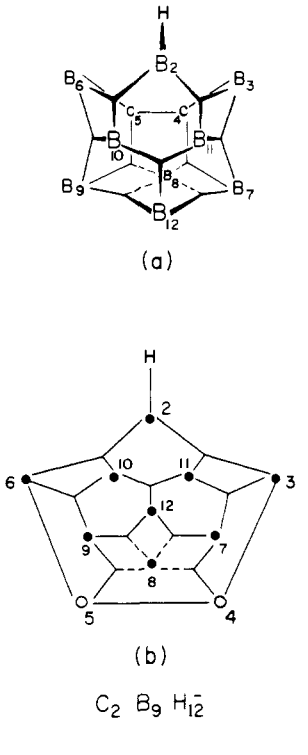

Figure 15. Localized valence structure for $C_2B_9H_{12}^-$: (a) three dimensional, (b) planar projection of the LMO's.

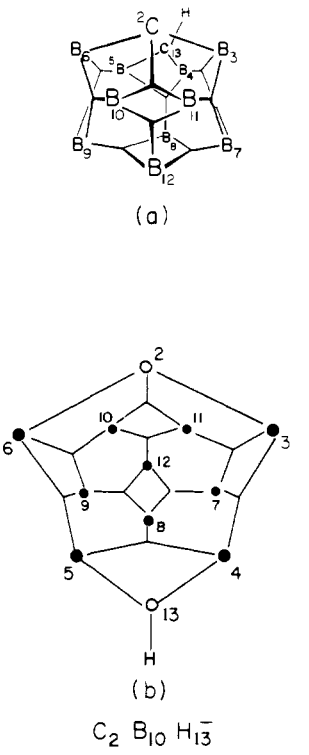

Figure 16. Localized valence structure for $C_2B_{10}H_{13}^-$: (a) three-dimensional, (b) planar projection of the LMO's.

center is B_8, which participates in five cage bonds and a BH_t bond. This center is extraordinary in that each cage bond has a population of ~0.4 e at B_8; in B_8H_{12}, the five cage bonds to B_1 (Figure 2) had quite unequal populations on B_1. Borons 10 and 11 are best described as nonfractional centers having small populations of 0.21 e in the 2-6 and 2-3 bonds, respectively. Finally we note that the B-H_b-B bonds are unsymmetrical and have populations of 0.60 e on B_4 or B_5 and 0.44 e on B_3 or B_6, qualitatively as expected from the respective B_4-H_{13} and B_3-H_{13} bond lengths (Table IV).

$C_2B_9H_{12}^-$. The LMO's (Figure 15) for $C_2B_9H_{12}^-$ are very similar to those in $B_{11}H_{13}^{2-}$, from which this ion formally can be obtained by (a) coalescence of the bridge hydrogens into the nuclei of atoms 4 and 5 to yield carbon atoms and (b) protonation at B_2. As a result of (a), the B-H_b-B bridges of $B_{11}H_{13}^{2-}$ are replaced by B-C two-center bonds, and a 4-5 two-center bond is found instead of the unsymmetrical 4-8-5 three-center bond. However, B_8 remains a fractional center. The protonation at B_2 removes an electron pair from the framework and induces changes in the bonding which are very similar to those discussed earlier for $B_9H_{14}^-$; here, the 2-10-11 bond of $B_{11}H_{13}^{2-}$ is lost, and in partial compensation the populations on B_{10} and B_{11} increase in the remaining framework bonds involving B_2.

$C_2B_9H_{12}^-$ is unique among the carboranes because of the possibility of migration of the extra terminal hydrogen at B_2 onto the open face. Indeed, this terminal hydrogen is quite far (1.33 Å) from B_2. Nevertheless, the bridging is apparently not well developed, as the populations on B_3 and B_6 in the localized orbital involving this hydrogen are only 0.19 e.

$C_2B_{10}H_{13}^-$. Like $B_{11}H_{13}^{2-}$ and $C_2B_9H_{12}^-$, the carborane ion $C_2B_{10}H_{13}^-$ also is based on an icosahedron missing a vertex. One carbon is placed in the uncapped ring of five heavy atoms while the other exists as a CH_2 group bridging the two borons in this uncapped ring which lie opposite to the ring carbon (Figure 16). The LMO structure is the (0, 10, 4, 0) structure predicted by Tolpin and Lipscomb[18] and displays the C_s point symmetry of the ion. The LMO's in $C_2B_{10}H_{13}^-$ are similar in appearance to those of $B_{11}H_{13}^{2-}$. The major differences are that B_8 is not a fractional center in $C_2B_{10}H_{13}^-$ and 3-4-7 and 6-5-9 bonds are found instead of B-H_b-B bridges. In addition the 2-3 and 2-6 bonds here show no appreciable donation to B_{11} and B_{10}. Finally, the CH_2 group is held in the bridging position by B-C single bonds, 4-13 and 5-13.

Summary

The PRDDO wave functions for B_8H_{14}, $B_8H_{13}^-$, $B_9H_{14}^-$, $B_{10}H_{13}^-$, $B_{11}H_{13}^{2-}$, $C_2B_7H_{13}$, $C_2B_9H_{12}^-$, and $C_2B_{10}H_{13}^-$ are analyzed in terms of the ground state charge distribution. These wave functions are the most accurate yet obtained for these molecules and are expected to be close to minimum basis set ab initio wave functions in accuracy.

Boys localized orbitals are presented for B_8H_{12}, B_8H_{14}, $B_8H_{13}^-$, B_9H_{15}, $B_9H_{14}^-$, $B_{10}H_{14}$, $B_{10}H_{14}^{2-}$, $B_{10}H_{13}^-$, $B_{11}H_{13}^{2-}$, $C_2B_7H_{13}$, $C_2B_9H_{12}^-$, and $C_2B_{10}H_{13}^-$. The localized orbitals are well behaved and result in the usual two-center B-B and B-H bonds and three-center B-H-B and B-B-B bonds. Fractional bonding is present in all compounds except B_8H_{14} and $C_2B_{10}H_{13}^-$. Comparisons of LMO's for molecules with similar structures have related changes in geometry and in the number of electrons available for framework bonding to resultant modifications in the LMO's, especially for those LMO's least well determined as judged from second-derivative test results.

Acknowledgments. We wish to thank the Office of Naval Research for support of this work.

References and Notes

(1) D. A. Kleier, T. A. Halgren, J. H. Hall, Jr., and W. N. Lipscomb, *J. Chem. Phys.*, **61**, 3905 (1974).
(2) C. Edmiston and K. Ruedenberg, *Rev. Mod. Phys.*, **35**, 467 (1963).

(3) (a) S. F. Boys, *Rev. Mod. Phys.*, **32**, 296 (1960); J. M. Foster and S. F. Boys, *ibid.*, **32**, 300 (1960); S. F. Boys, "Quantum Theory of Atoms, Molecules, and the Solid State", Per-Olov Löwdin, Ed., Academic Press, New York, N.Y., 1966, p 253.
(4) W. N. Lipscomb, *Acc. Chem. Res.*, **6**, 257 (1973).
(5) I. R. Epstein, D. S. Marynick, and W. N. Lipscomb, *J. Am. Chem. Soc.*, **95**, 1760 (1973).
(6) R. S. Mulliken, *J. Chem. Phys.*, **23**, 1833, 1841, 2338, 2343 (1955).
(7) R. J. Buenker and S. D. Peyerimhoff, *Chem. Phys. Lett.*, **3**, 37 (1969); *J. Chem. Phys.*, **45**, 3682 (1966).
(8) (a) T. A. Halgren and W. N. Lipscomb, *Proc. Nat. Acad. Sci. U.S.A.*, **69**, 652 (1972); (b) T. A. Halgren and W. N. Lipscomb, *J. Chem. Phys.*, **58**, 1569 (1973); (c) T. A. Halgren, D. A. Kleier, J. H. Hall, Jr., L. D. Brown, and W. N. Lipscomb, to be submitted.
(9) B_8H_{12}, R. E. Enrione, F. P. Boer, and W. N. Lipscomb, *Inorg. Chem.*, **3**, 1659 (1964).
(10) $B_8H_{13}^-$, R. Lewin, P. G. Simpson, and W. N. Lipscomb, *J. Chem. Phys.*, **39**, 1532 (1963). A bridging hydrogen was substituted for a bridging NH_2 group, in analogy with the relationship between B_2H_6 and $NH_2B_2H_5$ as described in this reference.
(11) B_9H_{15}, R. E. Dickerson, P. J. Wheatley, P. A. Howell, and W. N. Lipscomb, *J. Chem. Phys.*, **27**, 200 (1955).
(12) $B_9H_{14}^-$, N. N. Greenwood, J. A. McGinnety, and J. D. Owen, *J. Chem. Soc., Dalton Trans.*, 986 (1972).
(13) $B_{10}H_{14}^{2-}$, D. S. Kendall and W. N. Lipscomb, *Inorg. Chem.*, **12**, 546 (1973).
(14) $B_{10}H_{13}^-$, R. Schaeffer, private communication.
(15) $B_{11}H_{13}^{2-}$, C. F. Fritchie, *Inorg. Chem.*, **6**, 1199 (1967).
(16) D. Voet and W. N. Lipscomb, *Inorg. Chem.*, **6**, 113 (1967).
(17) M. R. Churchill and B. G. DeBoer, *J. Am. Chem. Soc.*, **96**, 6310 (1974).
(18) E. I. Tolpin and W. N. Lipscomb, *Inorg. Chem.*, **12**, 2257 (1973).
(19) $B_{10}H_{14}$, A. Tippe and W. C. Hamilton, *Inorg. Chem.*, **8**, 464 (1969).
(20) T. A. Halgren, R. J. Anderson, D. S. Jones, and W. N. Lipscomb, *Chem. Phys. Lett.*, **8**, 547 (1971), and references therein.
(21) Tables of molecular geometries are available from W.N.L.
(22) J. H. Hall, Jr., D. S. Marynick, and W. N. Lipscomb, *J. Am. Chem. Soc.*, **96**, 770 (1974).
(23) J. A. Pople and D. L. Beveridge, "Approximate Molecular Orbital Theory", McGraw-Hill, New York, N.Y., 1970.
(24) W. J. Hehre, R. F. Stewart, and J. A. Pople, *J. Chem. Phys.*, **51**, 2657 (1969); W. J. Hehre, R. Ditchfield, R. F. Stewart, and J. A. Pople, *ibid.*, **52**, 2191 (1970).
(25) (a) E. Switkes, R. M. Stevens, W. N. Lipscomb, and M. D. Newton, *J. Chem. Phys.*, **51**, 2085 (1969); (b) R. M. Stevens, *ibid.*, **52**, 1397 (1970).
(26) (a) E. A. Laws, R. M. Stevens, and W. N. Lipscomb, *J. Am. Chem. Soc.*, **94**, 4461 (1972); (b) D. S. Marynick and W. N. Lipscomb, *ibid.*, **94**, 8692 (1972).
(27) D. S. Marynick and W. N. Lipscomb, *J. Am. Chem. Soc.*, **94**, 8699 (1972).
(28) W. N. Lipscomb, "Boron Hydrides", W. A. Benjamin, New York, N.Y., 1963.
(29) D. A. Dixon, J. H. Hall, Jr., D. A. Kleier, T. A. Halgren, and W. N. Lipscomb, to be submitted.
(30) R. N. Grimes, "Carboranes", Academic Press, New York, N.Y., 1970.
(31) E. Switkes, W. N. Lipscomb, and M. D. Newton, *J. Am. Chem. Soc.*, **92**, 3847 (1970).
(32) I. R. Epstein and W. N. Lipscomb, *Inorg. Chem.*, **10**, 1921 (1971).
(33) Reference 28, p 59.
(34) (a) J. Dobson and R. Schaeffer, *Inorg. Chem.*, **7**, 402 (1968); (b) R. Schaeffer, Second International Meeting on Boron Chemistry, Leeds, England, May 1974.
(35) T. A. Halgren, I. M. Pepperberg, and W. N. Lipscomb, *J. Am. Chem. Soc.*, **97**, 1248 (1975).
(36) G. R. Eaton and W. N. Lipscomb, "NMR Studies of Boron Hydrides and Related Compounds", W. A. Benjamin, New York, N.Y., 1969, p 121.
(37) M. D. Newton, private communication.
(38) D. A. Dixon, D. A. Kleier, T. A. Halgren, and W. N. Lipscomb, *J. Am. Chem. Soc.*, **96**, 2293 (1974).
(39) F. E. Wang, P. G. Simpson, and W. N. Lipscomb, *J. Chem. Phys.*, **35**, 1335 (1961); *J. Am. Chem. Soc.*, **83**, 491 (1961).

Thermal Isomerization Studies of Small Metallocarboranes. Cage Rearrangement Equilibria and Reversible Cobalt Atom Migrations

Vernon R. Miller and Russell N. Grimes*

Contribution from the Department of Chemistry, University of Virginia, Charlottesville, Virginia 22901. *Received August 2, 1974*

Abstract: The vapor phase thermal behavior of six-, seven-, and eight-vertex monocobaltacarboranes, seven-, eight-, and nine-vertex dicobaltacarboranes, and a ten-vertex tricobaltacarborane was examined. In addition to phenomena of types previously observed in metallocarborane studies, e.g., intramolecular migration of metal and carbon atoms, and intermolecular transfer of cobalt and boron, several processes novel to metallocarborane chemistry were found, including the conversion of a neutral cobaltacarborane to a carborane via thermal ejection of cobalt, the migration of cobalt from a 5- to a 4-coordinate polyhedral vertex, and two examples of cage rearrangement equilibria involving reversible metal-metal cleavage. The isomerization of 1,7,2,3-$(\eta$-$C_5H_5)_2Co_2C_2B_3H_5$ to the 1,7,2,4 species via the isolable 1,2,4,5 and 1,2,3,5 intermediates was examined, and a mechanism has been proposed for the sequence. The equilibrium constant for the reversible rearrangement of 1,7,5,6- to 1,8,5,6-$(\eta$-$C_5H_5)_2Co_2C_2B_5H_7$ was determined as a function of temperature. The results obtained are discussed and evaluated in conjunction with previously reported work on the isomerization of large cobaltacarborane systems.

The rearrangement of polyhedral carboranes and metallocarboranes has received much attention from experimentalists and theoreticians.[1-6] Although the basic phenomenon involved—cooperative movement of atoms in the surface of a triangulated polyhedral cage—is almost unknown outside of boron chemistry, within this area it occurs with such facility and regularity that an understanding of it is a fundamental aspect of boron cage chemistry. Previous work on cage rearrangements has dealt with systems of large or intermediate size, especially those of icosahedral (12-vertex) geometry. The only reported small carborane rearrangement in the polyhedral $C_2B_{n-2}H_n$ series is that of octahedral 1,2- to 1,6-$C_2B_4H_6$.[7] In the metallocarborane field, Hawthorne et al. have examined the thermal isomerization of several monocobalt 9- to 13-vertex[4,5] and dicobalt 10- to 12-vertex[6] cages and noted several trends which we shall discuss later in this paper. Despite the isolation of many smaller metallocarboranes in recent years,[8] their thermal rearrangements have not previously been investigated.

In the course of our work on small metallocarboranes and metalloboranes having as few as five cage atoms,[9-11] we have noted numerous instances of thermal isomerization and/or disproportionation and accordingly initiated detailed studies of several selected cobaltacarborane systems having one to three metal atoms. The results are, in part, in accord with expectations based on studies of larger sys-